Scientific Research Publishing

Advances in Materials Physics and Chemistry, 2024, 14, 76-94
https://www.scirp.org/journal/ampc
ISSN Online: 2162-5328
ISSN Print: 2162-531X

Electrochemical Study of the Corrosion Inhibitory Capacity of Calcined Attapulgite in Reinforced Concrete Medium

Malang Bodian[1,2], Kinda Hannawi[2], Dame Keinde[3], Modou Fall[1], Aveline Darquennes[3], Prince William Agbodjan[2]

[1]Faculté des Sciences et Techniques, Département de Chimie, Université Cheikh Anta Diop de Dakar (Sénégal), Laboratoire de Chimie Physique Organique et d'Analyse Environnementales (LCPOAE), Dakar, Senegal
[2]Département de Génie Civil, Université de Rennes, INSA Rennes, Laboratoire de Génie Civil et Génie Mécanique (LGCGM), Rennes, France
[3]Département de Génie Civil, Université Cheikh Anta Diop, Ecole Supérieure Polytechnique de Dakar (Sénégal), Laboratoire de Matériaux de Génie Civil (LMGC), Dakar, Senegal
Email: bodianthomas@gmail.com, Kinda.Hannawi@insa-rennes, dkeinde85@yahoo.fr, modou.fall@ucad.edu.sn, aveline.darquennes@insa-rennes.fr, William.Prince-Agbodjan@insa-rennes.fr

How to cite this paper: Bodian, M., Hannawi, K., Keinde, D., Fall, M., Darquennes, A. and Agbodjan, P.W. (2024) Electrochemical Study of the Corrosion Inhibitory Capacity of Calcined Attapulgite in Reinforced Concrete Medium. *Advances in Materials Physics and Chemistry*, **14**, 76-94.
https://doi.org/10.4236/ampc.2024.145007

Received: March 16, 2024
Accepted: May 27, 2024
Published: May 30, 2024

Abstract

The durability of reinforced concrete structures is greatly influenced by the corrosion of the reinforcement. In addition to air pollution related to the repair of corroded structures, chloride ions are the main factors of corrosion of reinforced concrete structures. This study aims to valorize a clay inhibitor against reinforcement corrosion in reinforced concrete. This clay (Attapulgite) was incorporated into reinforced concretes at different percentages of substitution of calcined attapulgite (0%, 5% and 10%) to cement in the formulation. The corrosion inhibitory power of attapulgite is evaluated in reinforced concretes subjected to the action of chloride ions at different intervals in the NaCl solution (1 day, 21 days and 45 days) by electrochemical methods (zero current chronopotentiometry, polarization curves and electrochemical impedance spectroscopy). This study showed that in the presence of chloride ions, the composition based on 10% attapulgite has an appreciable inhibitory effect with an average inhibitory efficiency of 82%.

Keywords

Attapulgite, Electrochemical Methods, Inhibitor, Reinforced Concrete

1. Introduction

Reinforced concrete is today one of the most widespread building materials in

the world [1]. Therefore, controlling the factors that harm its durability becomes a necessity. Corrosion of steels in concrete is the main cause of deterioration and the most expensive in terms of maintenance. It is at the origin of many apparent defects which, if they do not generate losses of bearing capacity of the structure, prove harmful to the operation of the structure.

Numerous corrosion control methods for reinforced concrete structures have been applied to minimize the costs of corrosion [2] [3] [4] [5]. These include the use of corrosion inhibitors. Their use is considered to be the simplest and cheapest [6] and thus offers a cost-effective solution against steel corrosion. Calcium and sodium nitrites are the oldest inhibitors used in concrete. They were used as a preventive measure in new reinforced concrete structures (addition in tempering water). These products are found in many applications in the USA and Japan [7], where they have proven their effectiveness. Nitrites act as passivating agents because of their oxidizing properties [8]. They compete with chloride ions to reach the metal substrate, thus forming (and/or maintaining) the passive oxide layer according to reactions EQ.1 and EQ.2 [9] [10] [11]:

$$2Fe^{2+} + 2OH^{-} + 2NO^{2-} \rightarrow 2\ NO\uparrow + Fe_2O_3 + H_2O \quad (1)$$

$$Fe^{2+} + OH^{-} + NO^{2-} \rightarrow NO\uparrow + \gamma - FeOOH \quad (2)$$

The use of sodium nitrite was discontinued due to possible alkali reactions and its negative influence on the mechanical properties of concrete [12].

Since then, corrosion inhibitors to be added to concrete for the purpose of prevention or protection of existing structures have subsequently emerged. These inhibitors are also called migrant inhibitors (MCIs). The most used is monofluorophosphate (MFP). MFP (Na_2PO_3F) can be considered an anodic, cathodic or mixed inhibitor [7]. It is only applied to the concrete surface in the form of an aqueous solution with a percentage by mass between 10% and 20%. Indeed, MFP cannot be added at the time of tempering, because in addition to altering the mechanical properties of concrete, it causes a delay in setting [13]. The effectiveness of MFP is based both on its ability to diffuse in the porous network of concrete and its action on the surface of steel reinforcement [14]. In the poral solution of concrete, MFP reacts with calcium ions to form apatites, insoluble compounds of the formula $Ca_5(PO_4)_3X$ where the anion X can be OH^-, Cl^-or F^-, leading to the consumption of the active substance $PO3F^{2-}$ [15].

Although the use of these inorganic inhibitors in concrete led to positive results in terms of reducing the corrosion phenomenon by delaying its initiation, their toxicity effect limited their use in concrete [16]. Therefore, the need for more acceptable ecological materials has led scientists to use ecological inhibitors as alternatives for reinforced concrete. The use of clay materials as corrosion inhibitors for reinforced concrete then becomes an alternative due to their ecological aspect, non-toxic character, high availability and pozzolanic activity [17] [18].

Numerous studies [18] [19] have shown the positive influence of the use of clays as corrosion inhibitors for reinforced concrete by delaying the initiation of reinforcement corrosion. Work was carried out by Ahmed [18] on the develop-

ment of microreservoirs of corrosion inhibitors based on natural clay minerals for use as anti-corrosion fillers for mild steel in NaCl environment [18]. His studies focused on beidellite and palygorskite purified and modified by calcium or chitosan intercalation (CTS-NH_2). He showed that the functionalized clay mineral has a dual role: the release, at the interface, of heptanoate ions after their exchange by chloride ions from the aggressive medium, and the trapping of the latter. In our previous work, we were able to evaluate the corrosion inhibiting power of attapulgite for concrete reinforcing steel (high adhesion) in the interstitial solution of concrete synthesis by electrochemical methods [19].

Steel Fe500-3 in contact with the interstitial solution suffered an attack at a young age (3rd and 7th day of cure) in the absence of attapulgite. On the other hand, in the presence of attapulgite, steel Fe500-3 in the pore solution of mortar concretes is protected against corrosion at a young age (3rd and 7th days of cure) and at 28 days of maturation. However, it should be noted that the corrosion inhibitory power of clays in concrete is often studied in synthetic solutions representative of the concrete pore solution. They are also used for mild steel in NaCl medium. However, their inhibitory application as an addition in reinforced concrete remains very limited. It is therefore desirable to explore the possibility of using clay inhibitors by direct addition in the real environment of reinforced concrete.

The originality of this work consists in studying attapulgite (Senegalese clay) as a corrosion inhibitor, added directly in reinforced concrete by cement substitution.

For this purpose, cylindrical samples of reinforced concrete were made, some of which contain attapulgite. Attapulgite is added in reinforced concrete by substitution of 5 and 10% cement. The samples are then subjected to different operating conditions that promote the initiation and propagation of corrosion. First the specimens are immersed in an aggressive saline solution where corrosion is induced by chlorides, and thus corresponds to slow kinetic corrosion. Then, using a generator, the corrosion kinetics is accelerated by imposing an external current on the reinforcement of the test bodies kept immersed in the saline solution. At different times of these exposures, the state of the corrosion of the reinforcing bar in concrete will be analyzed by electrochemical measurements.

The results will make it possible to valorize attapulgite as a corrosion inhibitor for reinforced concrete. This is particularly important for Senegal and other countries that have a significant Atlantic coast (corrosion factor) and are full of significant amounts of this clay.

2. Experimental Protocol

2.1. Materials and Formulation

The study concrete is formulated with CEM I 52.5N cement, 0/4 sand, 4/10 gravel and tap water. Its basic mass composition is: sand 0/4 = 940 kg/m^3; gravel 4/10 = 1031 kg/m^3; cement = 270 kg/m^3 and a water/cement ratio = 0.65. This formulation is chosen so that the concrete has a low penetration resistance of Cl^-

ions and carbon dioxide. Some of them contain attapulgite with contents of 5 and 10% by substitution of the cement mass. However, due to the high water absorption capacity of attapulgite which can be up to 180% of its mass, this water is compensated in the formulation up to 100% of its mass. The reinforcement used in the manufacture of the reinforced concrete is hardened steel (high adhesion) with a diameter of 12 mm. Before their 90-day wet cure in water, resin is applied to the lower and upper parts of the overflowing reinforcement.

Attapulgite is introduced into reinforced concrete as a corrosion inhibitor. The clay comes from Pout (region of Thiès, Senegal), its centesimal chemical composition is: SiO_2 = 57, Al_2O_3 =13, Fe_2O_3 = 2, MgO = 14.4, Fire Loss = 11.4 and trace CaO [20].

Before its use in the formulation of reinforced concrete, attapulgite was ground into powder and sieved by an 80 μm fineness sieve, then calcined in an oven at 800˚C.

2.2. Corrosion Acceleration Techniques

After this 90-day wet cure, the test pieces for natural corrosion tests (immersed in a 0.5 M NaCl solution) and accelerated (by imposition of a current of 100 μA cm^{-2}) are partially dried at 45˚C for 14 days before being immersed in a corrosive solution of 0.5 M NaCl. The purpose of drying is to accelerate the penetration of chloride ions by a capillary absorption mechanism. The current density of 100 Ma cm^{-2} was chosen because it corresponds to the maximum value generally recorded in natural corrosion induced by chloride concentration [21]. The system consisting of the armature (working electrode connected to the positive pole of the generator) and the counter-electrode (stainless steel grid placed around the specimen and connected to the negative pole of the generator), is immersed in the electrolytic solution (NaCl 0.5 M). This solution is renewed as soon as its pH exceeds 10.

The test pieces that have undergone only the wet cure are designated TH 90D and constitute the reference test pieces. The other specimens are designated TS when they are simply immersed in the saline solution and EIC when they are immersed in the saline solution and subjected to the action of an external current (which accelerates corrosion).

At different times during these exposures of 1 day, 21 days and 45 days, the corrosion rate and inhibitory efficiency are measured via electrochemical measurements

2.3. Experimental Methods

The experimental device used for the electrochemical tests is shown in **Figure 1**. It comprises a Potentiostat/Galvanostat connected to an electrochemical cell and controlled by a computer equipped with the EC-Lab software. The cell consists of a saturated calomel reference electrode (ECS, +244 mV/ENH), a stainless steel grid used as a counter electrode and finally the steel bars in concrete as working electrodes. The reference electrode is placed on the grid via a wet sponge.

Measurements begin by monitoring the open-circuit free corrosion potential (OCP) until a balance is established after about 6 hours. Potentiodynamic bias measurements are then started by conducting a potential sweep around this OCP value in a potential range between −0.25 V and +0.25 V/OCP with a speed of 0.1 mV/s. Impedance measurements were performed at free corrosion potential with an amplitude of 50 mV. Potential scans are performed at variable frequencies in the range 1 Mhz - 10 mHz with 5 points/decade.

Electrochemical measurements are performed using a VSP BioLogic Science Instruments brand potentiostat/galvanostat, driven by the EC-Lab software, which allows the acquisition and processing of electrochemical data. The profile of the impedance diagrams generally recorded for reinforced concrete is shown in **Figure 2**.

The half-arc at high frequencies (HF) characterizes the resistance Rb which is assimilated to the total equivalent resistance of the liquid phase and the solid phase Gu *et al.* [23].

The semicircle at low and medium frequencies (LMF), is related to the capacity of the electrochemical double layer at the reinforcement surface, the charge transfer process and the diffusion process of ions in solution [24]. This semicircle (at LMF) then characterizes an electrochemical process (resistance to charge transfer/double electrochemical layer) that develops at the steel-concrete interface. This is why in the second block of the equivalent circuit (see **Figure 3**), a capacity associated with the double layer phenomenon (Cdc) is mounted in parallel with a load transfer resistance (Rtc) and a Warburg capacity (W) to take into account the phenomenon of diffusion [25].

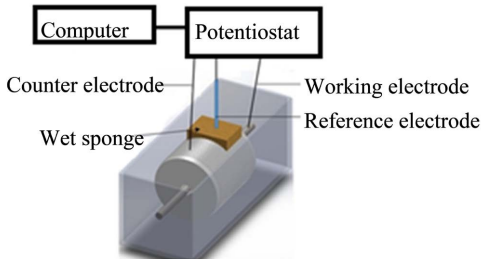

Figure 1. Electrochemical cell used for electrochemical testing.

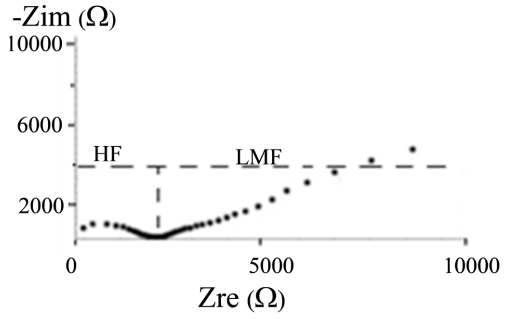

Figure 2. Profile of impedance diagrams of reinforced concrete [22].

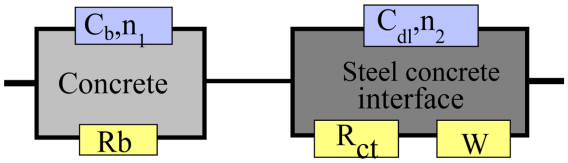

Figure 3. Equivalent circuit used to model impedance spectra.

The equivalent electrical circuit adopted for simulating electrochemical impedance diagrams is shown in **Figure 3**. It comprises a capacitor (C_b) dependent on the concrete's closed porosity, connected in parallel with the concrete's electrical resistance (R_b). This assembly is in turn connected in series with a second block comprising a double-layer capacitor (C_{dc}), connected in parallel with a charge transfer resistor (Rtc) and a Warburg capacitor (W). The double-layer and concrete capacities are determined from a constant-phase element (denoted EPC or Q) using the following equation [26]

$$C = \frac{(RQ)^{1/n}}{R} \tag{3}$$

The pseudo-capacitance Q is used to characterize the constant-phase element according to the values of the coefficient n and take into account the non-ideal behavior of the capacitance if its value is close to unity. The resistance Rb represents the total resistance of the liquid and solid phase [27].

The inhibitory efficiency (IE in %) is calculated from the polarization resistances according to the following formula [28]:

$$IE = \frac{R_{ih} - R_0}{R_{ih}} \times 100 \tag{4}$$

where:

- Rih, resistance in the presence of the inhibitor;
- Ro, resistance in the absence of inhibitor.

3. Results and Discussion

3.1. Corrosion Potential Monitoring

a) Natural corrosion in 0.5 M NaCl (TS specimens)

Figure 4 shows the evolution of reinforcement potential in concrete as a function of time after different stays in a saline solution, for different attapulgite additions to concrete at contents of 0 to 10% by cement. Corrosion potential values

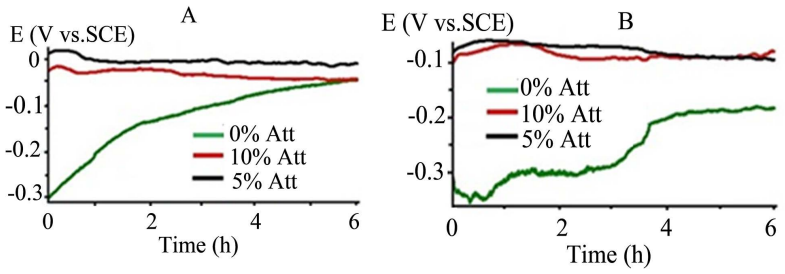

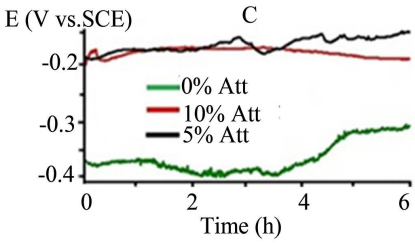

Figure 4. Monitoring the free corrosion potential of reinforcement in concretes with and without clay, immersed in saline solution: after 1 day (A), 21 days (B) and 45 days (C).

are determined after 6 h of potential monitoring. All corrosion potential values (E_{corr}) are given in relation to the saturated calomel electrode.

After 1 day in the salt solution (0% Att, 5% Att and 10% Att), the corrosion potentials measured after 6 h in the different compositions are of roughly the same order of magnitude. Values of −0.021 V/ECS for 5% Att, −0.044 V/ECS for 10% Att and −0.048 V/ECS for the control were recorded. These values show that the reinforcement in the concrete initially acquires a chemical protection provided by the high alkalinity of the embedding concrete [29] [30]. After 21 and 45 days in the saline solution (0% Att), it can be seen for each given composition that the corrosion potential becomes increasingly negative with increasing residence time of the reinforced concrete in the saline solution. This evolution of corrosion potentials towards negative values over time reflects the progressive depassivation of reinforcement in the concrete as the residence time of the specimens in the salt solution increases.

In the presence of 5% and 10% clay in the reinforced concrete, in contrast to the TS specimens without clay, the corrosion potential at 1 day, 21 days and 45 days in the saline solution becomes more positive as the clay content increases. This reflects corrosion protection of the reinforcement as attapulgite content increases.

b) Accelerated corrosion in 0.5 M NaCl (EIC specimens)

Figure 5 shows the evolution of curves representing free corrosion potential as a function of time, obtained at different times in the absence and presence of attapulgite in reinforced concrete subjected to corrosion acceleration by imposition of an external current.

When attapulgite is added to reinforced concrete, the corrosion potential is enhanced, irrespective of the time spent in the salt solution.

The evolution of the free potential after 1 day in the corrosive solution shows two distinct profiles depending on the substitution rate of clay in the reinforced concrete (0%, 5% and 10%). In the absence of attapulgite, the corrosion potentials of EIC specimens follow a pattern marked by a decrease in corrosion potential as a function of time. This initial decrease is generally observed when surface deposits are dissolved during polarization at zero intensity [31]. A quasi-stabilization of the OCP is observed after 4 hours of immersion. In the presence of 5% and 10% clay in the reinforced concrete, in contrast to the clay-free EIC control specimens, the corrosion potential after 1 day

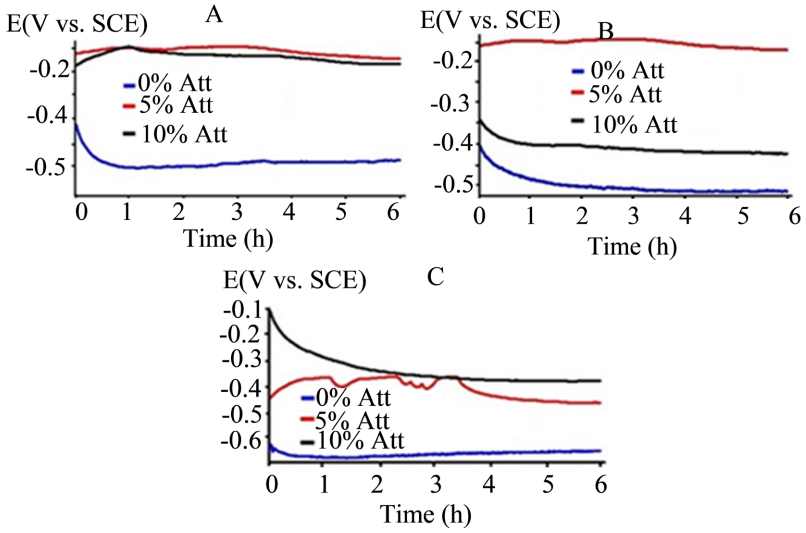

Figure 5. Monitoring the corrosion potential of specimens subjected to accelerated corrosion after galvanostatic polarization (100 μA cm^{-2}): after 1 day in salt solution (A), 21 days in salt solution (B) and 45 days in salt solution (C).

of acceleration in the saline solution becomes increasingly positive up to 2 h before stabilizing at around 6 h, characterizing the presence of a stable layer at the steel-concrete interface [32].

After 21 days under accelerated corrosion conditions, the reinforcement in concrete containing 5% attapulgite, as in the control, undergoes active corrosion, marked by a decrease in corrosion potentials as a function of time. Meanwhile, reinforcement in concrete containing 10% attapulgite remains protected against corrosion.

However, after 45 days under accelerated conditions, all specimens were found to be actively corroding. Disturbances were observed in the corrosion potentials of concrete reinforced with 10% clay, showing the formation of more or less porous corrosion products.

3.2. Potentiodynamic Polarization

a) Polarization in 0.5 M NaCl (TS specimens)

The polarization curves, plotted after 6 hours of free corrosion potential monitoring, are shown in Figure 6. Table 1 shows the various electrochemical parameters deduced from the polarization curves.

Figure 6 shows that, for each maturity, the addition of 10% clay to the concrete reduces the intensity of the anodic currents, but does not significantly modify the cathodic currents, in comparison with the control (TS). Furthermore, corrosion potential values are shifted towards noble values. This confirms the anodic character of the inhibitor and shows that the addition of clay to reinforced concrete reduces the rate of anodic dissolution of the metal, but does not affect the reduction reaction of dissolved oxygen in the concrete.

The anodic polarization curves after 1 day in salt solution show a shortening of the anodic branch as the proportion of cement in the specimens decreases

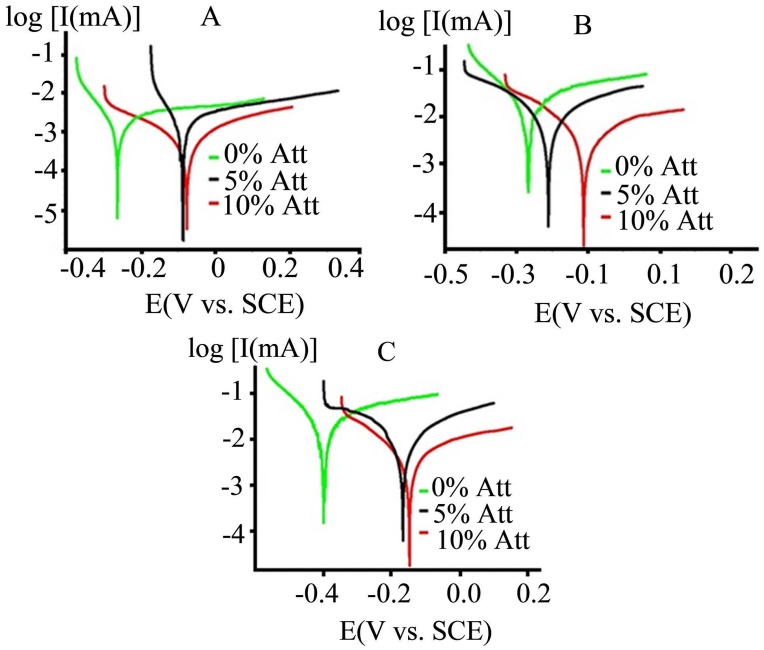

Figure 6. Tafel polarization curves for TS specimens with and without attapulgite: A: after 1 day; B: after 21 days and C: after 45 days in saline solution.

Table 1. Electrochemical parameters of natural corrosion: polarization resistance (R_p), corrosion potential (E_{cor}), corrosion current density (i_{cor}), coefficient of Tafel lines (β_a and β_c) and corrosion rate (V_{cor}) obtained from polarization curves..

	1 day			21 days			45 days		
	0% Att	5% Att	10% Att	0% Att	5% Att	10% Att	0% Att	5% Att	10% Att
R_p (kΩ·cm²)	230.1	305.9	1361.2	50.2	188.7	389.8	38.1	100.3	205.6
E_{cor} (mV)	−259.0	−88.9	−77.1	−268.4	−200.3	−108.7	−397.5	−198.3	−189.9
i_{cor} (µA/cm²)	0.06	0.04	0.03	0.40	0.17	0.16	0.80	0.50	0.44
βa (mV/dec)	79.9	118.5	307.3	102.1	393.4	309.6	140.2	337.1	372.9
Bc (mV/dec)	179.0	61.3	252.3	154.0	196.7	179.5	268.7	258.1	238.1
V_{cor} (µm/an)	0.7	0.3	0.4	4.7	2.3	2.0	9.1	6.5	5.2
EI (%)		24.7	83.1		73.4	87.1		62.0	81.4

(Figure 6(A)). Thus, anodic branches extending from −0.2 to 0.14 V/ECS for the control (0% Att), from −0.05 to 0.3 V/ECS for 5% clay and from 0.1 to 0.2 V/ECS for 10% attapulgite are noted. This confirms the results observed during corrosion potential monitoring, showing that the reinforcement is initially protected by the high alkalinity of the cement.

In addition, for each maturity, a decrease in corrosion current density (i_{cor}) was observed for all specimens containing attapulgite compared with the control

(Table 1). However, the 10% substitution of attapulgite for cement corresponds to the lowest current density at each maturity. A progressive increase in current densities as a function of specimen residence time in the solution containing Cl^- ions is also noted. Thus, Table 1 shows a corrosion current density of 0.4 µA cm^{-2} at 45 days, corresponding to low corrosion [33] [34] for 10% attapulgite substitution, 0.5 µA cm^{-2} for 5% substitution and 0.8 µA cm^{-2} for the control, corresponding to moderate corrosion [33]. Conversely to the variation in current density, the polarization resistance of clay-containing specimens is higher than that of the control (TS) for a given time. However, concrete reinforced with 10% attapulgite has the highest polarization resistance. As in the case of corrosion current densities, a progressive decrease in polarization resistance as a function of increasing salt solution residence time is also noted. Corrosion rates for specimens containing 10% clay are of the order of 5 µm/year at 45 days, corresponding to low corrosion [33]. For control specimens and those with 5% attapulgite, corrosion rates are between 5 and 10 µm/year, corresponding to moderate corrosion [33].

These results show that the passive film formed on the surface of the reinforcement after the manufacture of reinforced concrete gradually degrades when the interface is contaminated by chloride ions. This degradation is slowed down in the case of clay-reinforced concrete, which explains the reduction in corrosion current density in the presence of clay. A blocking of the anodic sites by a layer of mainly C-S-H (Hydrated Calcium Silicates) and additional C-A-S-H (Hydrated Alumina Calcium Silicates) [35] may account for this slowdown, as evidenced by the shift of corrosion potentials towards the anodic side in the presence of clay. It can also be explained by the fixation of chloride ions by the additional C-S-H and C-A-S-H formed with the pozzolanic reaction, thus reducing the contact time of chlorides with the reinforcement. When the specimens are immersed in the corrosive solution, the initial conditions at the steel-concrete interface gradually change in a direction favourable to the depassivation of the reinforcement. This explains the gradual increase in current densities for all specimens, as the time spent in the saline solution increases. Better corrosion inhibition was recorded for the 10% attapulgite-based composition, with an average inhibitory efficiency of 84%.

b) Polarization in 0.5 M NaCl with corrosion acceleration (EIC specimens)

Figure 7 shows the polarization and potentiodynamic curves of reinforcement in concrete with and without clay, recorded after 6h of corrosion potential monitoring at different times.

Figure 7 shows that, as in the case of natural corrosion, the presence of clay in the concrete induces a decrease in the anodic current and does not modify the cathodic reaction. What's more, its presence in the concrete shifts corrosion potentials towards less negative values. This confirms attapulgite's anodic character. The electrochemical parameters derived from these curves are shown in Table 2.

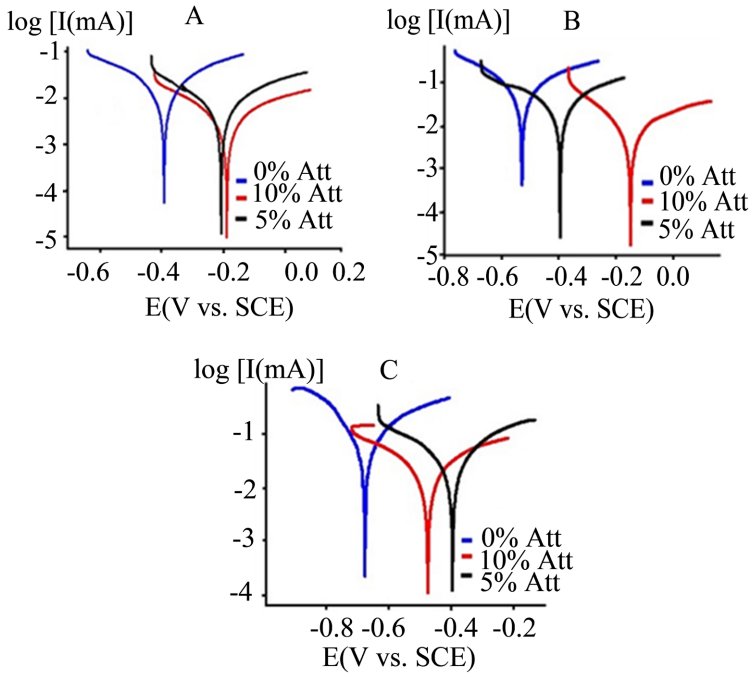

Figure 7. Polarization curves for EIC specimens with and without attapulgite: A: after 1 day, B: after 21 days and C: after 45 days of corrosion acceleration by applying a current density of 100 μA cm^{-2}.

Table 2. Electrochemical parameters of accelerated corrosion: polarization resistance (R_p), corrosion potential (E_{cor}), corrosion current density (i_{cor}), coefficient of Tafel lines (β_a and β_c) and corrosion rate (V_{cor}) obtained from polarization curves.

	1 day			21 days			45 days		
	0% Att	5% Att	10% Att	0% Att	5% Att	10% Att	0% Att	5% Att	10% Att
R_p (kΩ.cm^2)	20.4	177.4	343.0	17.6	40.4	143.4	12.4	34.2	58.5
E_{cor} (mV)	−391.7	−210.2	−189.8	−530.2	−398.8	−172.3	−672.5	−384.2	−471.8
i_{cor} (μA/cm^2)	0.64	0.25	0.13	1.81	1.25	0.31	2.80	1.37	0.85
βa (mV)	303.2	313.1	348.8	192.9	343.7	351.5	169.4	280.9	359.1
$-\beta$c (mV)	316.2	288.7	274.7	229.4	399.4	199.9	255.3	338.4	331.0
V_{cor} (μm/an)	7.42	2.83	1.58	21.21	14.59	2.89	30.71	16.17	9.92
EI (%)	Ref	88.5	94.0	Ref	56.4	71.8	Ref	63.7	78.8

Table 2 clearly shows that polarization resistances are higher in attapulgite-based concretes, and increase with the substitution rate. Corrosion current densities are also lower in clay-containing concretes. Currents are highest in the absence of clay and lowest at 10% substitution. Current densities recorded at 21 days on control specimens (1.81 μA/cm^2) and those with 5% clay (1.25 μA/cm^2) indicate rapid depassivation of reinforcement followed by active corrosion [33].

When 10% clay is added to reinforced concrete, the current density is less than 0.5 μA cm^{-2} at 21 days, indicating little corrosion. It is of the order of 0.8 Ma cm^{-2} after 45 days in salt solution, corresponding, according to Oelssner *et al.* [34], to moderate corrosion. These observations show that the addition of attapulgite to reinforced concrete can retard reinforcement corrosion. This is most pronounced with 10% substitution. This delay is confirmed by corrosion rate values. For example, the corrosion rate of specimens containing 10% clay is between 1 and 5 μm/year at 21 days, corresponding to low corrosion [33]. At 45 days, corrosion becomes moderate, with a rate equal to 9.92 μm/year for specimens with 10% attapulgite. On the other hand, for the control and with 5% attapulgite, corrosion rates are relatively high, exceeding 10 μm/year at 21 days. As in the case of natural corrosion, the 10% attapulgite composition showed better corrosion inhibition, with an average inhibitory efficiency of 82%.

3.3. Electrochemical Impedance Spectroscopy (EIS)

a) EIS in 0.5 M NaCl (EIC specimens)

Figure 8 shows the electrochemical impedance diagrams in the Nyquist plane of these specimens after 1-, 21- and 45-days' residence in saline solution (0.5 M NaCl). All the electrochemical parameters obtained from these impedance spectra are given in Table 3.

Analysis of these results shows that the impedance diagrams of the specimens have the same profile and present two distinct capacitive loops.

The half-arc at high frequencies (**HF**) is related to the porosity of the concrete, while the second loop, corresponding to low and medium frequencies (**LMF**), is attributed to the formation and growth of a film on the metal surface [36] [37] and the accompanying electrochemical reactions taking place at the steel-concrete interface. Figure 8 shows that, at high frequencies and for each given term, the semicircles characterizing the embedding concrete move away from the imaginary axis as the amount of clay in the concrete increases from 0 to 10%. This reflects an increase in the electrical resistivity of the concrete with the addition of clay. With increasing residence time, the semicircles move closer to the imaginary axis. For example, for 10% attapulgite, the real part of the impedance (Z_{re}) falls from 57.4 kΩ.cm^2 at 1 day to 18.5 kΩ.cm^2 at 21 days and 11.8 kΩ.cm^2 at 45 days. These results are consistent with a decrease in the electrical resistivity of concrete with specimen residence time. At low frequencies, the diameter of the arcs corresponding to electrochemical reactions is greater in the case of reinforced concretes containing clay.

Table 3 shows that the capacities of the concrete (C_b) and the double layer (C_{dl}) are lower in the case of concretes containing clay. In addition, the electrical resistance of the concrete (R_b) and the load transfer resistance (R_{tc}) are higher in reinforced concretes composed of clay. The decrease in C_b with the addition of attapulgite is linked to a decrease in the concentration of free chloride ions in the concrete's interstitial solution. This confirms clay's ability to reduce both the

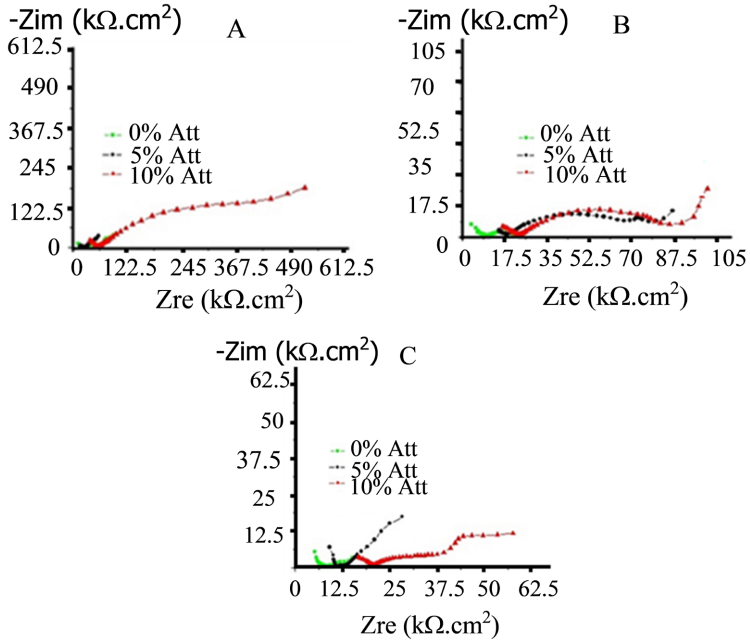

Figure 8. Electrochemical impedance diagrams of TS specimens with and without attapulgite: A: after 1 day in saline solution; B: after 21 days in saline solution; C: after 45 days in saline solution.

Table 3. Evolution of impedance parameters (R_b, C_b, C_{dl}, R_{tc}, n) at different times in saline solution.

	1 day			21 days			45 days		
	0% Att	5% Att	10% Att	0% Att	5% Att	10% Att	0% Att	5% Att	10% Att
R_b (kΩ.cm²)	22.8	24.3	55.1	5.3	17.5	18.8	10.0	11.1	14.6
C_b (10^{-11}F/cm²)	75.5	4.6	3.5	150.4	8.1	5.7	263.9	8.4	6.5
n_1	0.789	0.822	0.895	0.720	0.693	0.662	0.703	0.998	0.646
C_{dl} (10^{-5} F/cm²)	16.8	13.0	9.0	154.1	15.1	9.6	495.4	20.3	18.6
n_2	0.381	0.370	0.539	0.427	0.523	0.357	0.411	0.463	0.559
R_{tc} (kΩ.cm²)	41.9	75.6	574.8	1.3	26.0	37.5	11.4	15.1	34.7
W (μF/cm²)	2.27	0.47	2.63	16.60	6.66	4.34	3.70	3.45	4.54
EI (%)	Ref	44.63	92.67	Ref	95.04	96.51	Ref	24.49	67.15

permeability of chloride ions in concrete through chloride ion binding and electrochemical reactions at the steel-concrete interface. However, the electrical and charge-transfer resistances of the concrete decrease progressively with the length of time the reinforced concrete remains in the saline solution.

These observations are in line with Tafel's electrochemical polarization parameters, confirming a progressive change in the initial conditions of the steel-concrete interface in a direction favorable to reinforcement depassivation as the

residence time of the specimens in the corrosive solution increases. Values of the empirical coefficient n_1 relating to the surface of reinforcement in concrete range from 0.646 to 0.999. In these cases, the EPC can be assimilated to a pure capacity, the deviation from unity reflecting surface in homogeneities [38]. In the case of empirical coefficients n2 relating to the steel-concrete interface, the values are rather close to 0.5 indicating a diffusional process. The inhibitory efficiency index indicates better corrosion inhibition for the 10% attapulgite-based composition, with an average inhibitory efficiency of 85%.

The images presented in Figure 9 show the state of reinforcement in concretes with and without clay after a 45-day stay in the NaCl solution. The images reveal a progressive loss of the passive white layer protecting the reinforcement in the case of specimens containing no clay.

b) EIS in 0.5 M NaCl after corrosion acceleration (EIC specimens)

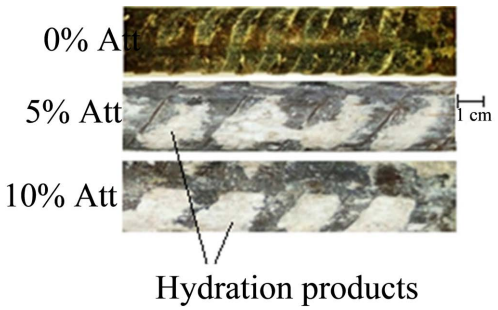

Figure 9. Images of concrete reinforcement in the presence and absence of attapulgite after splitting at 45 days.

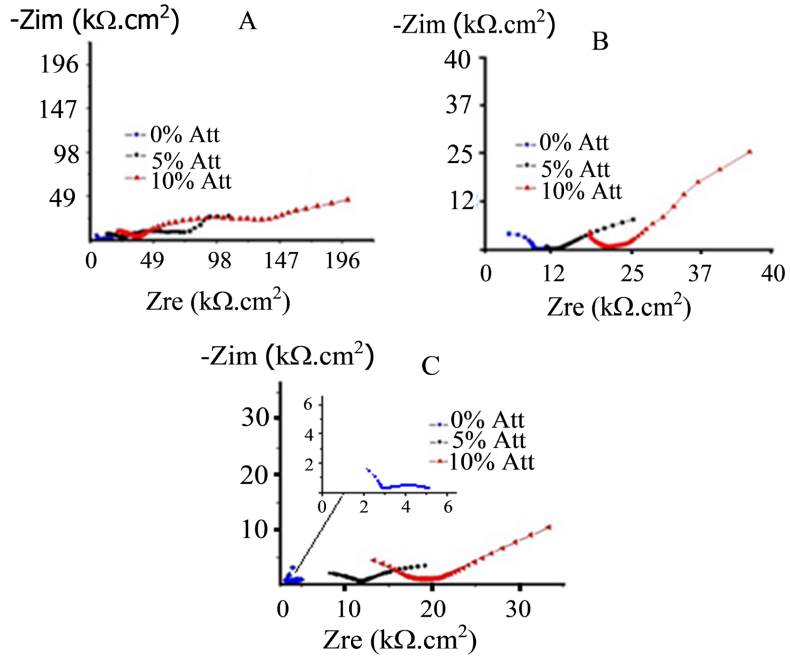

Figure 10. Electrochemical impedance spectra of specimens with and without attapulgite: A: after 1 day, B: after 21 days and C: after 45 days of corrosion acceleration by applying a current density of 100 μA cm^{-2}.

Table 4. Evolution of electrochemical parameters of accelerated corrosion (R_b, C_b, C_{dl}, R_{tc}) at different timescales.

	1 day			21 days			45 days		
	0% Att	5% Att	10% Att	0% Att	5% Att	10% Att	0% Att	5% Att	10% Att
R_b (kΩ.cm²)	7.53	24.45	34.77	8.52	10.04	18.13	3.15	8.05	13.18
C_b (10^{-11} F/cm²)	276.70	2.44	1.15	109.90	2.63	1.33	60.11	8.59	4.43
n_1	0.704	0.561	0.648	0.926	0.815	0.970	0.995	0.656	0.730
C_{dl} (10^{-2} F/cm²)	15.43	0.90	0.62	5.64	1.05	0.57	0.70	1.29	1.02
n_2	0.239	0.483	0.505	0.100	0.230	0.468	0.346	0.123	0.129
R_{tc} (kΩ.cm²)	23.1	67.6	117.1	8.0	16.0	32.1	5.1	9.3	18.7
W (F/cm²)	0.41	0.02	0.02	0.12	0.09	0.03	2.71	0.04	0.04
EI (%)	Ref	65.83	80.34	Ref	50.04	75.12	Ref	45.16	72.82

Impedance diagrams recorded after the application of external current to specimens with and without attapulgite are reproduced in Figure 10. The curves are similar to those recorded for natural corrosion.

As in the case of natural corrosion, Figure 10 shows that, at each maturity, the semicircles that characterize the high-frequency range of clay-reinforced concrete are further away from the imaginary axis. At low frequencies, the diameter of the arcs corresponding to electrochemical reactions is greater in the case of reinforced concrete containing clay. The electrochemical parameters derived from the simulation of these spectra are shown in Table 4.

Table 4 shows that, as in the case of natural corrosion, the electrical resistance of concrete (R_b) and charge transfer resistance (R_{tc}) increase as the substitution rate of clay in concrete rises from 0 to 10%. Conversely, the electrical capacities of concrete (C_b) and double layer (C_{dl}) decrease when the substitution rate of clay in concrete increases from 0 to 10%.

Comparison of the values obtained for natural corrosion (Table 3) and accelerated corrosion (Table 4) showed that, for a given percentage of clay in the concrete, R_b and R_{ct} resistances are lower in the case of accelerated corrosion, implying higher electrical conductivity due to strong chloride ion penetration and accelerated corrosion at the steel-concrete interface for EIC specimens.

The results also show that C_b values at a given clay percentage are lower in the case of accelerated corrosion. This reflects the greater presence of corrosion products injected into the pores of the embedding concrete. The same applies to C_{dc} values, explaining the more pronounced formation of a corrosion layer at the steel-concrete interface.

The images presented in Figure 11 show the condition of reinforcement in concrete in the presence and absence of clay after 45 days under accelerated corrosion conditions.

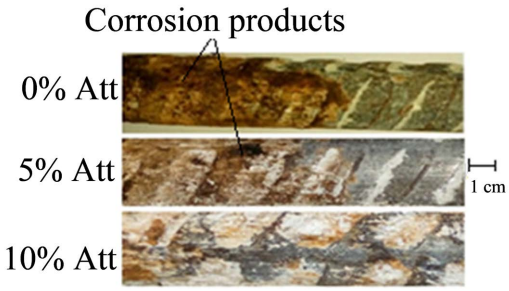

Figure 11. Images of concrete reinforcement in the presence and absence of attapulgite after splitting at 45 daysin corrosion acceleration by applying a current density of 100 μA cm^{-2}.

The condition of the reinforcement showed a more pronounced development of corrosion on the reinforcement of the control specimens (EIC 45 J) and with 5% clay, to the detriment of the passive layer protecting the reinforcement.

3.4. Attapulgite Corrosion Inhibition Mechanism

Attapulgite has an appreciable inhibiting power at 10% substitution. Its corrosion-inhibiting effect is explained by the physical adsorption at the steel-concrete interface of a layer (the white layer observed on reinforcement) made up mainly of C-S-H and C-A-S-H, resulting from the reaction between attapulgite and portlandite from cement hydration, according to equations EQ.5 and EQ.6.

$$\text{Silica}\left(\text{Attapulgite}\right)+\text{Portlandite}\left(\text{cement}\right)\rightarrow \text{C-S-H}$$

$$\text{C-S-H}+\text{Al}\left(\textit{Attapulgite}\right)\rightarrow \text{C-A-S-H}$$

These hydration products (C-A-S-H) improve the chemical binding capacity of chlorides to the cementitious matrix, notably through the production of Friedel salts, and reduce the diffusivity of the material towards chlorides [39].

This layer also inhibits anodic sites, which explains the behavior of anodic slopes and the decrease in doubling capacity in the presence of attapulgite.

4. Conclusions

This work examines the corrosion-inhibiting power of attapulgite added directly to reinforced concrete using electrochemical analytical methods.

The electrochemical results of the study of reinforcement corrosion in concrete in the presence of attapulgite showed that when corrosion takes place in the presence of chlorides under natural corrosion conditions, the presence of attapulgite in concrete increases the initiation time of reinforcement corrosion. This inhibitory effect was most pronounced when 10% of the cement was replaced by clay, with a satisfactory effectiveness of around 84%. Under accelerated corrosion conditions, electrochemical results showed that concretes composed with 5% attapulgite corroded at the same rate as the control, with zero inhibitory effectiveness. On the other hand, with the addition of 10% attapulgite, we noted a slowdown in corrosion compared with the control and the 5% atta-

pulgite concrete, with a satisfactory inhibiting power of around 82%.

Conflicts of Interest

The authors declare no conflicts of interest regarding the publication of this paper.

References

[1] Oesterlee, C., Sadouki, H. and Brühwiler, E. (2008) Analyse structurale d'un pont composé de BFUP et de béton armé. Ecole Polytechnique Fédérale de Lausanne, Lausanne, 133-140.

[2] Courard, L. and Bissonnette, B. (2016) Réparation des ouvrages en béton armé-Partie 2: Compatibilité et performances. Analyse Chimique et Caractérisation. Techniques de l'Ingénieur. https://doi.org/10.51257/a-v1-c6302

[3] Duprat, F., Sellier, A. and Lacarrière, L. (2004) Evaluation probabiliste du risque de corrosion par carbonatation. *Revue Française de Génie Civil*, **8**, 975-997. https://doi.org/10.1080/12795119.2004.9692637

[4] Soufi, A. (2013) Etude de la durabilité des systèmes béton armé: mortiers de réparation en milieu marin. Doctoral Dissertation, Université de La Rochelle, La Rochelle.

[5] Arteaga, E.-B., Schoefs, F. and Capra, B. (2010) Contribution à une gestion durable de structures en béton arme soumises à la pénétration d'ions chlorure. *Congrès LM17: Maîtrise des Risques et sûreté de fonctionnement*, La Rochelle, 1-10.

[6] Bhawna, C., Kumar, T.-P. and Jyoti, B.-H. (2022) Corrosion Inhibition by Aluminum Oxide. In: Verma, C., Aslam, J., and Hussain, C.M., Eds., I*norganic Anticorrosive Materials*: *Past*, *Present and Future Perspectives*, Elsevier, Amsterdam, 231-249. https://doi.org/10.1016/B978-0-323-90410-0.00013-1

[7] Andrade, C., Alonso, C., Acha, M. and Malric, B. (1992) Preliminary Testing of Na_2PO_3F as a Curative Corrosion-Inhibitor for Steel Reinforcements in Concrete. *Cement and Concrete Research*, **22**, 869-881. https://doi.org/10.1016/0008-8846(92)90111-8

[8] Dhouibi, L., Triki, E., Salta, M., Rodrigues, P. and Raharinaivo, A. (2003) Studies on Corrosion Inhibition of Steel Reinforcement by Phosphate and Nitrite. *Materials and Structures*, **36**, 530-540. https://doi.org/10.1007/BF02480830

[9] Soeda, K. and Ichimura, T. (2003) Present State of Corrosion Inhibitors. *Cement & Concrete Composites*, **25**, 117-122. https://doi.org/10.1016/S0958-9465(01)00058-0

[10] Rincon, O.-T., Perez, O., Paredes, E., Caldera, Y., Urdaneta, C. and Sandoval, I. (2002) Long-Term Performance of ZnO as a Rebar Corrosion Inhibitor. *Cement & Concrete Composites*, **24**, 79-87. https://doi.org/10.1016/S0958-9465(01)00029-4

[11] Chakri, S. (2015) Compréhension des mécanismes d'inhibition de la corrosion des armatures métalliques des bétons par des molécules d'origine biologique. Doctoral Dissertation, Université Pierre et Marie Curie-Paris VI, Paris.

[12] Berke, N.S. and Sundberg, K.M. (1990) Effects of Calcium Nitrite and Microsilica Admixtures on Corrosion Resistance of Steel in Concrete. *Special Publication*, **122**, 265-280.

[13] Rivetti, M.L.S., Netto, J., Junior, M.A. and Ribeiro, D.V. (2018) Corrosion Inhibitors for Reinforced Concrete. Corrosion Inhibitors, Principles and Recent Applications, 35-58.

[14] Chaussadent, T., Nobel-Pujol, W., Farcas, F., Mabille, I. and Fiaud, C. (2006) Effec-

tiveness Conditions of Sodium Monofluorophosphate as a Corrosion Inhibitor for Concrete Reinforcements. *Cement and Concrete Research*, **36**, 556-561. https://doi.org/10.1016/j.cemconres.2005.09.006

[15] Andrade, C. and Alonso, C. (1996) Corrosion Rate Monitoring in the Laboratory and Onsite. *Construction and Building Materials*, **10**, 315-328. https://doi.org/10.1016/0950-0618(95)00044-5

[16] Agboola, O., Kupolati, K.W., Fayomi, O.S.I., Ayeni, A.O., Ayodeji, A., Akinmolayemi, J.J. and Oluwasegun, K.M. (2022) A Review on Corrosion in Concrete Structure: Inhibiting Admixtures and Their Compatibility in Concrete. *Journal of Bio- and Tribo-Corrosion*, **8**, 25.

[17] Ahmed, I., Karim, E. and Kadri, E.-H. (2010) Etude des déformations de retrait d'un mortier contenant différentes additions minérales. "*SICZS*_2010" *Symposium International sur la Construction en Zone Sismique*, Algérie, 26-27 October 2010, 1-10.

[18] Ahmed, A.-A. (2014) Argiles en tant que Réservoirs d'Inhibiteurs de Corrosion métallique issus de ressources naturelles dans des peintures pour la protection des métaux (ARIC). Thèse de cotutelle entre l'université de lorraine et l'Université Cadi Ayyad, Université de Lorraine, Duché de Lorraine.

[19] Bodian, M., Keinde, D., Touré, A.-O., Gueye, P.-M. and Fall, M. (2018) Valorization of Pout Attapulgite as Corrosion Inhibitor for Fe500-3 Concrete Reinforcing Iron in the Interstitial Solution of Concrete. *International Journal of Innovation and Applied Studies*, **24**, 1603-1613.

[20] Benaissa, M., Bendani, K., Belas, N., Belguesmia, K., Missoum, H., *et al.* (2016) Effet de l'ajout de la bentonite sur les propriétés des mortiers et des bétons autoplaçants. *Matériaux & Techniques*, **104**, Article No. 608. https://doi.org/10.1051/mattech/2017021

[21] Isabelle, V.-F. (2009) Sensibilité de la technique d'émission acoustique à la corrosion des armatures dans le béton. Thèse de Doctorat, Université de Toulouse, Toulouse.

[22] Hikmat, A.H. (2008) Applicabilite et efficacite d'une protection galvanique aux aciers de precontrainte. Thése de Doctorat, Université de Toulouse, Toulouse.

[23] Gu, P., Ellott, S., Hristova, R., Beaudoin, J.J., Brousseau, R. and Baldock, B. (1997) A Study of Corrosion Inhibitor Performance in Chloride Contaminated Concrete by Electrochemical Impedance Spectroscopy. *ACI Materials Journal*, **49**, 385-395.

[24] Ford, S.J., Shane, J.D. and Mason, T.O. (1998) Assignment of Features in Impedance Spectra of the Cement-Paste/Steel System. *Cement and Concrete Research*, **28**, 1737-1751. https://doi.org/10.1016/S0008-8846(98)00156-2

[25] Nasser, A. (2010) La corrosion des aciers dans le béton à l'état passif et par carbonatation: Prise en compte des courants galvaniques et des défauts d'interface acier-béton. Thèse de doctorat, Université de Toulouse, Toulouse.

[26] Ryou, J., Voigt, T., Konsta-Gdoutos, M.S., Varacalle, D.J., Mason, T. and Shah, S.P. (2005) Corrosion Resistance of Functionally Graded Coatings on Plain Steel Rebars. *Journal of Advanced Concrete Technology*, **3**, 69-75. https://doi.org/10.3151/jact.3.69

[27] Cerdán, C.-E., Blasco-Tamarit, E., García-García, D.-M., García-Antón, J., Akid, R. and Walton, J. (2013) Effect of Temperature on Passive Film Formation of UNS N08031 Cr-Ni Alloy in Phosphoric Acid Contaminated with Different Aggressive Anions. *Electrochimica Acta*, **111**, 552-561. https://doi.org/10.1016/j.electacta.2013.08.040

[28] Doubi, M., Dermaj, A., Ramli, H., Chebabe, D., Hajjaji, N. and Srhir, A. (2013)

Inhibition de la corrosion d'un acier E24 dans des eaux d'irrigation agricole. *Science Lib Editions Mersenne, Mersenne*, **5**, 2111-4706.

[29] Capra, B. (2014) Construction et travaux publics, Vieillissement, pathologies et réhabilitation du bâtiment. Techniques de l'Ingénieur Réf, C6151 V1.

[30] Hu, J.Y., Zhang, S.S., Chen, E. and Li, W.G. (2022) A Review on Corrosion Detection and Protection of Existing Reinforced Concrete (RC) Structures. *Construction and Building Materials*, **325**, Article 126718.

[31] Sherif El-Sayed, M., Potgieter, J.H., Comins, J.D., Cornish, L., Olubambi, P.A. and Machio, C.N. (2009) The Beneficial Effect of Ruthenium Additions on the Passivation of Duplex Stainless Steel Corrosion in Sodium Chloride Solutions. *Corrosion Science*, **51**, 1364-1371. https://doi.org/10.1016/j.corsci.2009.03.022

[32] Joanna, E., Takenouti, H., Saadi, B.A. and Taibi, S. (2020) Electrochemical Studies of Steel Rebar Corrosion in Clay: Application to a Raw Earth Concrete. *Corrosion Science*, **168**, Article 108556. https://doi.org/10.1016/j.corsci.2020.108556

[33] ASTM C8 76-91 (1991) Standard Test Method for Half Cell Potentials of Reinforcing Steel in Concrete. Annual Book of ASTM Standards.

[34] Oelssner, W., Berthold, F. and Guth, U. (2006) The iR Drop—Well-Known but Often Underestimated in Electrochemical Polarization Measurements and Corrosion Testing. *Corrosion and Materials*, **57**, 455-466.
https://doi.org/10.1002/maco.200603982

[35] Bodian, M., Keinde, D., Yade, I., Hannawi, K., Agbodjan, P.-W., Fall, M. and Darquennes, A. (2022) Study of Attapulgite as an Additive in Reinforced Concrete by Substitution of Cement and Its Effects on the Durability Properties of Hardened Concrete. *Open Journal of Civil Engineering*, **12**, 301-319.
https://www.scirp.org/journal/ojce
https://doi.org/10.4236/ojce.2022.123018

[36] Cairns, J. and Abdullah, R. (1995) An Evaluation of Bond Pullout Tests and Their Relevance to Structural Performance. *Structural. Engineer*, **1**, 179-185.

[37] Soda, K. and Takao I. (2003) Present State of Corrosion Inhibitors in Japan. *Cement and Concrete Composites*, **25**, 117-122.
https://doi.org/10.1016/S0958-9465(01)00058-0

[38] Garcés, P., Saura, P., Méndez, A., Zornoza, E. and Andrade, C. (2008) Effect of Nitrite in Corrosion of Reinforcing Steel in Neutral and Acid Solutions Simulating the Electrolytic Environments of Micropores of Concrete in the Propagation Period. *Corrosion Science*, **50**, 498-509. https://doi.org/10.1016/j.corsci.2007.08.016

[39] Thomas, M.D.A., Hooton, R.D., Scott, A. and Zibara, H. (2012) The Effect of Supplementary Cementitious Materials on Chloride Binding in Hardened Cement Paste. *Cement and Concrete Research*, **42**, 1-7.
https://doi.org/10.1016/j.cemconres.2011.01.001